AIAA JOURNAL
Vol. 32, No. 2, February 1994

Technical Notes

TECHNICAL NOTES are short manuscripts describing new developments or important results of a preliminary nature. These Notes cannot exceed 6 manuscript pages and 3 figures; a page of text may be substituted for a figure and vice versa. After informal review by the editors, they may be published within a few months of the date of receipt. Style requirements are the same as for regular contributions (see inside back cover).

Performances of Riblets in the Supersonic Regime

E. Coustols* and J. Cousteix†
CERT/ONERA, 31055 Toulouse, France

I. Introduction

THE widely known ability of riblet surfaces to reduce turbulent skin friction has been well-demonstrated for the last two decades. The effectiveness of riblets, narrow, streamwise, microgrooved surfaces, has been tested under a variety of conditions: in the subsonic as well as the transonic regimes, with nonzero pressure gradients, and for two- or three-dimensional external flows.[1–3] Because of the current concerns of some industrial manufacturers, a long-term experimental research program dealing with turbulent drag reduction using such passive devices has been pursued at CERT/ONERA since 1986.[3–7] The encouraging results of this research have allowed us, as well as the Aerodynamics Branch of ONERA/Chatillon, to be directly involved in the successful flight tests carried out by Airbus Industrie and its partners in October 1989.[8]

Thus, as mentioned previously, numerous experimental studies have investigated the potential of riblets for decreasing turbulent friction drag and have shown that the optimum groove shapes have a sharp peak protruding into the flow and a height h and spacing s typically of the order of 12–15 viscous lengths. For optimum flow conditions, maximum drag reductions up from 6% to 8% have been reported in subsonic as well as transonic flows.[1,3,9]

The way such grooves alter the turbulent friction is not exactly understood, although a great amount of data has been recorded; because of the microgeometry of these devices, boundary-layer measurements or spectral analysis inside these grooves are very difficult, but they are possible.[10] Furthermore, several attempts to calculate such manipulated external as well as internal flows have been reported[3]; the results they gave are often contradictory. Nevertheless, direct numerical simulations of turbulent flows over riblets have been recently performed[11] and could help in understanding the basic physics.

Today, there is a rebirth of interest in a long-range supersonic transport aircraft[12] and drag reduction should surely be investigated. One of the possible approaches could be the supersonic application of riblets.[13] Thus, in collaboration with Aérospatiale, an investigation has been recently carried out in the ONERA/Modane-Avrieux S2 wind tunnel to ascertain the effectiveness of riblets at different freestream Mach numbers: 1.6, 2.0, and 2.5.

Besides the first tests conducted in the Cambridge tunnel by Squire and Savill on possible modification of shock-boundary layer interaction due to riblets,[14] only a few studies have been performed at supersonic conditions. First of all, Robinson analyzed the effects of V-shaped grooves ($s/h = 1$, $h = 0.15$ mm, $h_w^+ = h\sqrt{(\tau_w/\rho_w)}/\nu_w = 17$) on turbulence structure at a Mach number of 2.97 and a unit Reynolds number ($Re_{l=1m}$) of 15×10^6 (Ref. 15). No measurement of drag variation was made; however, the experiments revealed important decreases in the turbulence intensity in the near-wall region and a noticeable thickening of the viscous sublayer. Later on, Gaudet looked at the performances of a riblet surface ($s/h = 1$, $h = 0.051$ mm) at a freestream Mach number of 1.25 and $Re_{l=1m}$ from 2.4×10^6 up to 11.0×10^6 (Ref. 16). Skin friction measurements were performed using a drag balance set into the side wall of the Royal Aircraft Establishment Bedford wind tunnel. Maximum reductions of the order of 7% were obtained. Gaudet also looked at the effect of flow misalignment with respect to the rib direction. Lastly, Walsh[1] and Bushnell[13] mentioned unpublished flight experiments conducted at the NASA Dryden and NASA Langley research centers at Mach numbers up to 2.0, for symmetric V-shaped grooves ($s/h = 1$, $h = 0.033$ mm and 0.076 mm).

II. Experimental Facilities and Test Conditions

The experiments were performed in the supersonic S2 facility; the dimensions of the test section are 1.93 m height and 1.75 m width. The model was comprised of a cylindric portion, the length and diameter of which are 1.565 m and 0.090 m, respectively, with an upstream conical nose of 0.437 m length. The tip half-angle of 6 deg as well as the dimensions of the model were chosen to minimize the shock wave generation as well as to maximize the percentage of friction contribution to the drag budget from the cylinder.

The model was mounted along the axis of the test section at angles of attack and yaw equal to zero. Shadowgraphs allowed the researchers to verify that the shock at the nose did not reflect on the model, but on the sting for all flow conditions. Tests were performed at three freestream Mach numbers, M_∞, of 1.6, 2.0, and 2.5 for various stagnation pressures varying between 0.50–1.40 bar or 1.55 bar (this maximum value depends upon M_∞). The stagnation temperature was kept constant at approximately 300 K. These test conditions lead to a unit Reynolds number range $Re_{l=1m} = 4.9$–22.3×10^6.

The boundary layer was tripped at 20 mm downstream of the conical tip using a carborundum band, the average height of which is 203 μm. Lastly, it should be noted that transition tripping was optimized for $M_\infty = 2.5$ and $Re_{l=1m} = 4.9 \times 10^6$ and overestimated for the other conditions.

The riblet models were supplied by the 3M Company and machined in a thin sheet of adhesive backed vinyl. Their aspect ratio s/h is constant and equal to 1; three depths were considered: $h =$ 0.033, 0.051, and 0.076 mm. The models were placed along the constant radius part of the centerbody, with the grooves aligned with the freestream. The cylinders on top of which the riblet material was fastened had a smaller diameter (89.8 mm), so that only the grooves were protruding into the flow to avoid any forward-step disturbance. The leading edge of the vinyl sheets was set at 6.4 mm downstream of the cone-cylinder junction, which corresponds to 87% of the wetted area of the model covered with riblet material.

Drag variations were estimated from an internal, one-component drag balance. The reference smooth cylinder was equipped with 19 pressure taps, while the conical nose had two sets of 4 pressure taps at 90 deg intervals in the azimuthal direction. These latter taps, located at 10 mm and 417 mm downstream of the conical tip, allowed the researchers to ascertain whether the model was set at zero angles of attack and yaw. Several pressure taps were also placed at the base of the model and inside the cavity, between the sting and the inner cylinder.

Received April 5, 1993; revision received Aug. 20, 1993; accepted for publication Aug. 23, 1993.

*Research Engineer, Aerothermodynamics Department.
†Professor, Head of Aerothermodynamics Department. Senior Member AIAA.

III. Experimental Results

The pressure distributions along the model, for $M_\infty = 2.0$ are plotted in Fig. 1 ($X = 0$ refers to the cone-cylindric portion junction). The static pressure is constant on the conical nose. There is rather good agreement between the measured values and the theoretical one ($Cp = 0.0466$ for $M_\infty = 2.0$). Downstream of the cone-cylindric portion junction, there is a velocity increase due to the flow expansion. The values of the pressure ratio could be estimated using the two-dimensional Prandtl-Meyer formulation. Further downstream, the flow decelerates towards the cylinder base. It should be noted that small streamwise irregularities of Cp along the cylinder are reported. They are attributed to freestream oscillations previously observed in this supersonic test section. However, those irregularities induce relative variations of the local Mach numbers of less than 1%. The Reynolds number does not have too much effect on the pressure distribution; the higher the Reynolds number is, the smaller the pressure coefficient along the cylinder is.

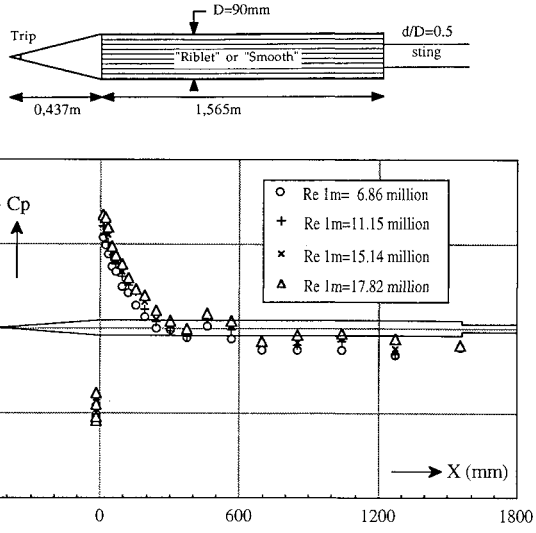

Fig. 1 Pressure distributions for $M_\infty = 2.0$.

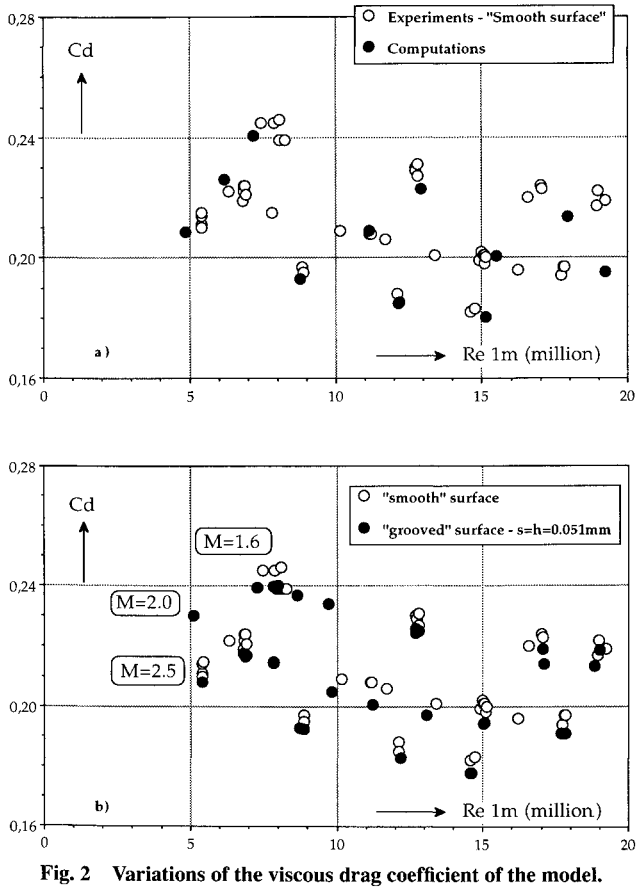

Fig. 2 Variations of the viscous drag coefficient of the model.

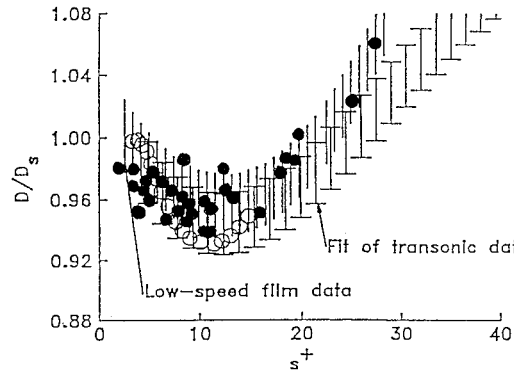

Fig. 3 Synthesis of skin friction drag data.

For different freestream conditions, the internal drag balance furnishes the total drag force, including the base drag as well as the pressure force acting upon the internal cylinder of the model. These last two forces are estimated from the pressure measurements; their contribution is not negligible in the drag budget: 13% and 24%, respectively, of the total measured drag (there is a very slight dependence on the Reynolds number). Substracting those pressure forces from the measured total drag, the net viscous drag force of the model is then obtained.

The values of the viscous drag coefficient of the reference model (smooth surface) are plotted vs $Re_{l=1m}$ for the three values of M_∞ in Fig. 2a; the reference surface is the projected surface. In that diagram, the values of the computed drag coefficients, using an integral boundary-layer method, are also given. Considering assumptions made to perform the calculations (no shock wave and no overthickening at the transition tripping, no pressure evolution along the cylinder, etc.) the agreement between the computed and estimated values of Cd is rather good since the difference does not exceed 4%.

Furthermore, Fig. 2a shows an excellent reproductibility of the drag measurements. In fact, the greatest scatter occurs for the low Reynolds number range, which corresponds to very small forces in comparison to the drag capacity. These discrepancies could be attributed to scatter on measurements of the remaining, aforementioned pressure forces. Nevertheless, the uncertainties of the drag coefficient of the model estimated from crude values given by the internal dynamometer do not exceed 1.6%. Thus, the expected magnitude of the drag reduction due to grooved surfaces will be greater than that which could be accounted for by the experimental error.

When the constant radius cylinder portion is covered with riblets, the pressure coefficient on the conical nose, at the model base or in the inner cavity, does not vary within the experimental uncertainty. It is therefore reasonable to believe that smooth-grooved surface comparisons were performed under the same test conditions. An example of the results is given in Fig. 2b, for the model: $h = 0.051$ mm. The net overall drag decreases are obtained over the whole Reynolds number range.

IV. Discussion and Conclusion

Plots identical to the previous one could be drawn for the other two riblet models: $h = 0.033$ mm and 0.076 mm. Maximum net total viscous drag reductions up to 4% are reported. At $M_\infty = 2.0$ and 2.5, net drag decreases are recorded for all of the riblet heights considered. However, at $M_\infty = 1.6$, increases are observed for unit Reynolds numbers greater than 15 million.

The aforementioned Mach and Reynolds numbers dependence could be avoided when plotting results using the nondimensionalized riblet height h_w^+. This parameter varies with respect to the streamwise coordinate because of the slight favorable pressure gradient and the Reynolds effect; but, its average value, integrated

all along the manipulated area, would be representative of the rib geometry for given test conditions. The explored Mach numbers and stagnation pressure ranges allowed variations of the $\overline{h_w^+}$ parameter from 2 to 31.

Computations based on the integral method showed that the friction contribution of the manipulated area was almost independent of the freestream conditions and equal to 65% of the total drag of the model. The variations of the friction drag coefficient of the manipulated area are plotted vs $\overline{h_w^+}$ in Fig. 3, taken from Walsh and Anders.[9] Such a representation allows us to gather together the results, even though some scatter is observed; the latter is not due to the Mach number but could be attributed to the extreme sensitivity of drag decreases to cross section uniformity, surface finition, etc.

Hence, these supersonic results are compared with Gaudet's data and both the low-speed film data and the fit of transonic data. It should be noted that for $\overline{h_w^+} < 20$, drag decreases are obtained while increases are recorded for higher values; maximum friction drag reductions occur for $\overline{h_w^+}$ close to 10. The drag reducing benefits are comparable to those recorded earlier by several investigators at different speeds. Thus, our supersonic data fit perfectly with the other data, provided that the rib height is scaled with the variables taken at the wall.

Acknowledgments

The authors wish to acknowledge the "Service Technique des Programmes Aéronautiques" for supporting this study and 3M-France for providing the riblet material. They are also grateful to the whole team from the ONERA/Modane-Avrieux S2 wind tunnel.

References

[1]Walsh, M. J., "Riblets," *Viscous Drag Reduction in Boundary Layers*, edited by D. M. Bushnell and J. N. Hefner, Progress in Astronautics and Aeronautics, AIAA, Washington, DC, 1990, pp. 203–261.

[2]Savill, A. M., "Drag Reduction by Passive Devices: A Review of Some Recent Developments," *Structure of Turbulence and Drag Reduction*, edited by A. Gyr, International Union of Theoretical and Applied Mechanics Symposium (Zürich, Switzerland), Springer-Verlag, Berlin, 1990, pp. 429–465.

[3]Coustols, E., and Savill, A. M., "Turbulent Skin Friction Drag Reduction by Active and Passive Means," AGARD Rept. 786, 1992.

[4]Coustols, E., "Behaviour of Internal Manipulators: Riblet Models in Subsonic and Transonic Flows," AIAA Paper 89-0963, March 1989.

[5]Coustols, E., and Cousteix, J., "Experimental Investigation of Turbulent Boundary Layers Manipulated with Internal Devices: Riblets," *Structure of Turbulence and Drag Reduction*, edited by A. Gyr, International Union of Theoretical and Applied Mechanics Symposium (Zürich, Switzerland), Springer-Verlag, Berlin, 1990, pp. 577–584.

[6]Coustols, E., and Cousteix, J., "Experimental Manipulation of Turbulent Boundary Layers in Zero Pressure Gradient Flows Through External and Internal Devices," *Proceedings of the Seventh Symposium on Turbulent Shear Flows* (Stanford, CA), Vol. 2, 1989, Paper 25-3.

[7]Coustols, E., and Schmitt, V., "Synthesis of Experimental Riblet Studies in Transonic Conditions," *Turbulence Control by Passive Means*, Fluid Mechanics and its Applications, edited by E. Coustols, Kluwer, Dordrecht, The Netherlands, 1990, pp. 123–140.

[8]Robert, J. P., "Drag Reduction: An Industrial Challenge," AGARD Rept. 786, 1992.

[9]Walsh, M. J., and Anders, J. B, Jr., "Riblet/LEBU Research at NASA Langley," *Applied Scientific Research*, Vol. 46, No. 3, 1989, pp. 255–262.

[10]Benhalilou, M., Anselmet, F., Liandrat, J., and Fulachier, L., "Experimental and Numerical Investigation of a Turbulent Boundary Layer over Riblets," *Proceedings of the Eighth Symposium on Turbulent Shear Flows* (Munich, Germany), Vol. 1, 1991, Paper 18-5.

[11]Choi, H., Moin, P., and Kim, J., "Direct Numerical Simulation of Turbulent Flow over Riblets," Stanford Univ. CTR Manuscript 137, Stanford, CA, July 1992.

[12]Poisson-Quinton, Ph., "A French Look at the Future Supersonic Transport," International Aerospace Symposium, Nagoya, Japan, 1992, ONERA TP 1992-209.

[13]Bushnell, D.M., "Supersonic Aircraft Drag Reduction," *Proceedings of the AIAA 21st Fluid Dynamics, Plasmadynamics and Lasers Conference* (Seattle, WA), AIAA, Washington, DC, June 1990.

[14]Squire, L. C., and Savill, A. M., "Some Experiences of Riblets at Transonic Speeds," *Proceedings of the Turbulent Drag Reduction by Passive Means Conference* (London), Vol. 2, Sept. 1987, pp. 392–407.

[15]Robinson, S. K., "Effects of Riblets on Turbulence in a Supersonic Boundary Layer," AIAA Paper 88-2526, June 1988.

[16]Gaudet, L., "Properties of Riblets at Supersonic Speeds," *Applied Scientific Research*, Vol. 46, No. 3, 1989, pp. 245–254.

Vortex Breakdown over Delta Wings in Unsteady Freestream

Ismet Gursul*
University of Cincinnati, Cincinnati, Ohio 45221
and
Chih-Ming Ho†
University of California, Los Angeles, Los Angeles, California 90024

Introduction

VORTEX breakdown is an intriguing phenomenon that has been observed both on delta wings and in tubes. Compared with the internal flows in tubes, the major difference of the leading-edge vortex over a delta wing is the continuous feeding of vorticity from the leading edge. In the early studies of vortex breakdown over steady delta wings, flow visualization was used extensively to observe the effects of geometric parameters such as angle of attack, sweep, and yaw angle.[1,2] For a summary of observations and related interpretations, the reader is referred to the reviews of Wedemeyer,[3] Lee and Ho,[4] and Rockwell.[5] The observations in tube experiments and different explanations of the phenomena based on instability, wave propagation, and flow stagnation are summarized in several review articles.[6–8]

The observations over steady delta wings and in tubes showed that there are two important parameters affecting vortex breakdown location: *swirl angle* [$\phi = \tan^{-1}(v/u)$, where v and u are the swirl and axial components of velocity, respectively] and *external pressure gradient* outside the vortex core. An increase in the swirl angle or in the magnitude of adverse pressure gradient causes the breakdown location to move upstream. For a leading-edge vortex, the swirl angle is related to the wing geometry such as angle of attack and sweep angle. It was shown that an increase in angle of attack or aspect ratio corresponds to an increase in swirl angle.[4] The streamwise pressure gradient on the suction surface of the wing is an adverse one due to the existence of a trailing edge, and its magnitude depends on angle of attack and sweep angle. For unsteady wings, both the swirl angle and the pressure gradient are expected to vary in time during a maneuver.

In this study, vortex breakdown characteristics over stationary delta wings in an unsteady freestream were investigated. Breakdown may occur over the wing with increasing unsteadiness even when no breakdown is observed over the wing in steady freestream at the same angle of attack. Experiments were conducted on two delta wings (aspect ratio $A = 1$ and 2). The characteristics of breakdown and its time-dependent behavior were documented by flow visualization and laser Doppler anemometer (LDA) measurements.

Experimental Facility

Experiments were conducted in a vertical unsteady water channel with a cross-sectional area of 45.7 × 45.7 cm. The freestream

Presented as Paper 93-0555 at the AIAA 31st Aerospace Sciences Meeting, Reno, NV, Jan. 11–14, 1993; received Jan. 14, 1993; revision received Sept. 9, 1993; accepted for publication Sept. 13, 1993.

*Assistant Professor, Department of Mechanical, Industrial, and Nuclear Engineering. Member AIAA.

†Professor, Mechanical, Aerospace, and Nuclear Engineering Department. Member AIAA.